A frequency-domain procedure to design TMDs for lively pedestrian structures considering Human-Structure Interaction

Christian Gallegos-Calderón[a,*], Carlos M. C. Renedo[a], M. Dolores G. Pulido[a,b], Iván M. Díaz[a]

[a] *E.T.S.I. Caminos, Canales y Puertos, Universidad Politécnica de Madrid, Calle del Profesor Aranguren 3, 28040, Madrid, Spain*
[b] *Instituto de Ciencias de la Construcción Eduardo Torroja, Consejo Superior de Investigaciones Científicas, Calle Serrano Galvache 4, 28033, Madrid, Spain*

Abstract

The use of advanced low-density high-strength materials, such as Fibre Reinforced Polymers (FRPs) or aluminium alloys, has enabled to construct lightweight and slender footbridges, which structural design may be governed by the Vibration Serviceability Limit State (VSLS) under human-induced loads. These structures may be excited in resonance by higher and less energetic harmonics of human actions in contrast to footbridges built with traditional construction materials. Additionally, Human-Structure Interaction (HSI) may be relevant on the dynamic response of these type of pedestrian structures. A solution for the aforementioned issues may be the installation of Tuned Mass Dampers (TMDs) in the bridge. Thus, this paper presents a frequency-domain procedure to design TMDs for lively pedestrian structures based on a coupled human-structure-controller system. The proposal,

*Corresponding author
Email address: christian.gallegos@upm.es (Christian Gallegos-Calderón)

which accounts for uncertainties associated to the structure and the interaction phenomenon, is applied to design passive inertial control systems for an FRP footbridge. Also, the implications of HSI in the design of TMDs are discussed, and the performance of the designed devices is assessed considering two human actions, bouncing and walking. Since the peak value of the steady-state response of a pedestrian structure can be fast assessed through algebraic operations, the proposed approach is suitable to design robustly control systems against human-induced vibrations. As a result, structural elements and controllers can be properly dimensioned, leading to further cost-effective footbridge projects.

Keywords: Human-Structure Interaction, lightweight pedestrian structures, vibration control, Tuned Mass Dampers, frequency domain

1. Introduction

The innovation in construction techniques and the use of non-conventional materials, such as Fibre Reinforced Polymers (FRPs) or aluminium alloys, in modern pedestrian structures may lead to undesired human-induced vibrations. Due to the low effective modal masses of these type of structures, resonant responses may not only be associated to the first harmonic of pedestrian loads. In fact, higher and less energetic harmonics of human actions have been found to excite vibration modes with natural frequencies above 5 Hz in aluminium footbridges [1] and FRP pedestrian structures [2]. Recently, Russell et al. [3] achieved a good agreement between experimental and numerical results in a Glass-FRP (GFRP) footbridge, whose first vertical vibration mode is at 15.10 Hz, when a force model with frequency content

up to about 17 Hz was employed to describe the human load. An accurate assessment of lightweight footbridges at Vibration Serviceability Limit State (VSLS) is required since this limit state may govern the structural design, especially for FRP pedestrian structures [4].

Another important aspect in the dynamic behaviour of lightweight footbridges is Human-Structure Interaction (HSI) since this phenomenon contributes to a significant reduction of the vertical acceleration response [5]. HSI may be even more relevant in FRP structures as the pedestrian-to-structure mass ratio is much higher than those typically considered for concrete or steel footbridges. To account for the interaction phenomenon, models considering the dynamic parameters of the human body have been used as alternatives to the moving force models found in Boniface et al. [6], Butz et al. [7] or ISO [8]. For instance, Single Degree-of-Freedom (SDOF) Mass-Spring-Damper (MSD) systems have been employed to represent the action of walking humans in the vertical direction [9, 10, 11]. Inverted Pendulum systems have also been employed to characterize the action of humans [12]. However, the latter leads to results that contradict experimental observations and presents time-varying non-linear mechanisms, which are complicated to implement in daily engineering practice [5].

Similarly to walking, SDOF MSD systems have been proposed to investigate the interaction phenomenon in structures with people bouncing [13]. As feet remain in contact with the structure at any instant, the dynamic parameters of structure may be affected by HSI. Another model to represent a pedestrian bouncing is the SDOF Mass-Spring-Damper-Actuator (MSDA) system [14, 15]. The actuator force affects both, the human body

and the structure, and is described by a typical Fourier series. The load coefficients of this force are referred as Generated Load Factors (GLFs), which are not the standard Dynamic Load Factors (DLFs) commonly stated in design guidelines. Although the aforementioned models are usually employed in time-domain analyses, frequency-domain methods may be preferable since human-induced vibrations are inherently governed by harmonic excitations.

Regarding the control of human-induced vibrations in footbridges, a Tuned Mass Damper (TMD) has proven to be the most widespread solution to this issue [7]. The main advantage of this system is its purely mechanical functioning. Nevertheless, the device is inefficient to control vibrations in a range of frequencies due to the presence of uncertainties or responses involving several vibration modes of the structure [16]. Also, when the TMD is mistuned, its control effect is drastically degraded. In order to increase the frequency band of effectiveness and the robustness under uncertainties, a Multi-TMD (MTMD) [17] or a semi-active TMD [18] may be employed as suitable so-lutions in pedestrian structures. Although some mistuning issues may arise in an MTMD, its advantage is that the passive nature of the control system is kept, so no power supply is required. Moreover, when one of the units of a MTMD fails or is vandalized, the other ones remain functioning, assuring always a response reduction of the structure. Currently, several experimental and numerical studies of TMDs oriented to mitigate human-induced vibra-tions in footbridges are available in literature [19, 20, 21].

When dealing with footbridges built with non-conventional materials and susceptible to HSI, classical methods to design inertial controllers may not be directly applicable as the structure may not be longer modelled as a de-

terministic SDOF system with negligible damping. In this sense, a general frequency-domain procedure to design TMDs for lively responsive pedes-trian structures is proposed in this paper. The novelty of this approach is the consideration of uncertainties associated to the structure and the in-teraction phenomenon to design passive inertial controllers. From the un-certainties defined by probabilistic distributed functions, stochastic coupled human-structure systems are generated, and the controller is robustly de-signed for all them simultaneously. Hence, the effects related to the device mistuning are minimized. The proposal is based on a multi-objective opti-mization problem, which accounts for the minimization of the H_∞ norm of a sum of closed-loop Transfer Functions (TFs) and the cost of the control system. The first objective considers the TFs of stochastic coupled human-structure-controller systems, whereas the second objective is represented by the total inertial mass of the device. The proposed procedure is applied to obtain the parameters of a TMD and a MTMD for an all-FRP footbridge, which is considered to be at the design stage. Additionally, the performance of the designed controllers is assessed considering two pedestrian actions, bouncing and walking. This methodology allows that VSLS requirements are met through the implementation of vibration controllers instead of over dimensioning the structure.

The remainder of this paper is organized as follows. All the elements to derive the coupled human-structure-controller system are explained in Section 2, and the proposed frequency-domain procedure to design TMDs is presented in Section 3. The benchmark FRP footbridge together with the de-sign load scenarios are described in Section 4. Whilst the inertial controllers

are designed and assessed in Section 5. In Section 6, the performance of the designed control systems are investigated considering pedestrians bouncing at midspan and walking across the bridge. Finally, the main conclusions and some future work are presented in Section 7.

2. System modelling

In this work, a system comprised of three elements (structure, humans, and inertial controllers) is adopted. If pedestrians performing bouncing on the structure are considered, a Linear Time-Invariant (LTI) system can be assumed. As a result, a fully frequency-domain analysis of the dynamic problem is allowed, taking advantage of a total closed-loop TF. Fig. 1a shows a representation of the coupled human-structure-controller system, in which the structure is depicted as a SDOF system for the sake of illustration.

2.1. Closed-Loop Scheme

The closed-loop TF of the human-structure-controller coupled system between the footbridge acceleration ($\ddot{x}_s$) and the human driving force (F_a) is named G_{CL} herein. This TF is graphically represented with a dashed-line box in the block diagram shown in Fig. 1b, and it is mainly characterized by two feedback loops associated to the HSI and the TMDs.

The closed-loop TF of the human-structure-controller system, derived from Fig. 1b in the Laplace domain may be expressed as follows

$$G_{CL}(s) = \frac{G_S(s) \cdot G_H(s)}{1 + G_S(s) \cdot \Big(G_{HSI}(s) + G_T(s) \Big)} \tag{1}$$

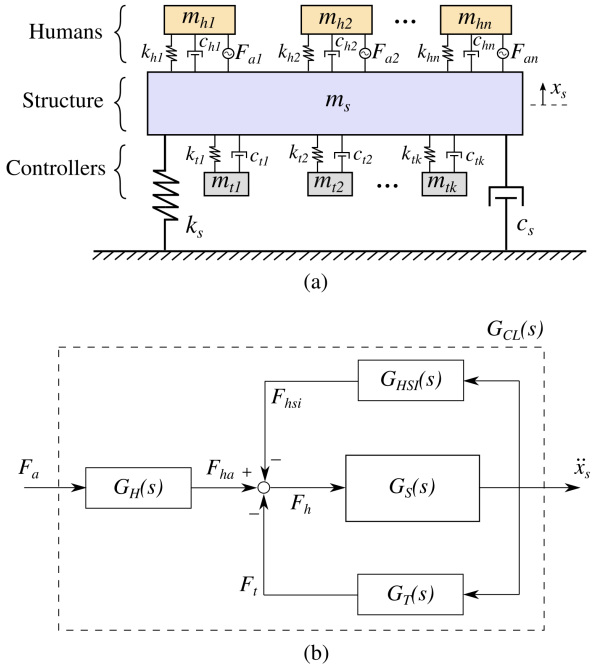

Figure 1: System modelling: (a) Coupled human-structure-controller system, and (b) Block diagram.

where $s = j\omega$ is the Laplace variable, ω (rad/s) is the angular frequency, $G_S(s)$ is the TF of the structural system, $G_H(s)$ is the TF between the human driving force and the contact force of the human with the structure, $G_{HSI}(s)$ is the TF associated to HSI, and $G_T(s)$ is the TF related to the controller-structure interaction. These TFs are described in the following subsections.

2.2. Structure system

For the system of the structure, each vibration mode can be represented through a MSD system, defined by the effective modal mass, m_s (kg), and natural frequency, f_s (Hz), which can be directly obtained from a numerical

model. Additionally, the damping ratio, ζ_s, is required, so its value may be assumed according to the material and layout of the structure using recommendations provided in existing guidelines. The TF of the structure is

$$G_S(s) = \frac{s^2 X_s(s)}{F_h(s)} = \sum_{i=1}^{N_s} \frac{1/m_{si}\, s^2}{s^2 + 2\,\omega_{si}\,\zeta_{si}\, s + \omega_{si}^2} \tag{2}$$

with $i = 1, 2, \ldots\ N_s$, where N_s is the number of considered vibration modes of the structure, $\omega_{si} = 2\pi f_{si}$ (rad/s) is the angular natural frequency of the ith mode of the structure. Also, $F_h(s)$ is the Laplace transform of the applied force acting on the structure and $s^2 X_s(s)$ is the Laplace transform of the structural acceleration, where $X_s(s)$ denotes the Laplace transform of the structural displacement.

2.3. Human system

A SDOF MSDA system is selected to represent a person while accounting for HSI. The pedestrian is defined by means of the body mass m_h (kg), natural frequency f_h (Hz) and damping ratio ζ_h. Also, a harmonic force generated by the human legs, usually known as human driving force (F_a), is accounted for via a pair of action-reaction forces acting simultaneously on both the footbridge and the person.

The TF between F_{ha}, which is the force generated by the humans without including the force transmitted to them due to the structure movement, and F_a is as follows

$$G_H(s) = \frac{F_{ha}(s)}{F_a(s)} = \sum_{n=1}^{N_h} \frac{-s^2}{s^2 + 2\,\omega_{hn}\,\zeta_{hn}\, s + \omega_{hn}^2} \tag{3}$$

with $n = 1, 2, \ldots\ N_h$, where N_h is the number of people acting at the control location, $\omega_{hn} = 2\pi f_{hn}$ (rad/s) is the angular frequency of the body of the

nth pedestrian, and ζ_{hn} is the associated damping ratio of the nth human. Regarding, F_a, which is the input force to G_{CL}, it can be expressed as follows

$$F_a = W_h \sum_{r=1}^{R} \mathrm{GLF}_r \sin(r\, 2\pi f_a + \varphi_r) \tag{4}$$

where W_h is the weight of the person, R represents the number of considered harmonics, f_a is the excitation frequency of the pedestrian action, and φ_r is the phase angle associated to the rth harmonic.

Additionally, a TF between the human interacting force (F_{hsi}), which is the force transmitted due to the structure movement, and $\ddot{x}_s$ appears, and it is expressed as follows

$$G_{HSI}(s) = \frac{F_{hsi}(s)}{s^2 X_s(s)} = \sum_{n=1}^{N_h} \frac{m_{hn}\,(2\,\omega_{hn}\,\zeta_{hn}\,s + \omega_{hn}^2)}{s^2 + 2\,\omega_{hn}\,\zeta_{hn}\,s + \omega_{hn}^2} \tag{5}$$

2.4. Inertial controller system

When dealing with TMDs, the control force (F_t) entering the structural system is obtained from the transmitted force of each inertial controller (Fig. 1a). This force is the sum of the transmitted force of every TMD within the MTMD system. Hence, the TF between F_t and $\ddot{x}_s$ is as presented below

$$G_T(s) = \frac{F_t(s)}{s^2 X_s(s)} = \sum_{k=1}^{N_t} \frac{m_{tk}\,(2\,\omega_{tk}\,\zeta_{tk}\,s + \omega_{tk}^2)}{s^2 + 2\,\omega_{tk}\,\zeta_{tk}\,s + \omega_{tk}^2} \tag{6}$$

with $k = 1, 2, \ldots\ N_t$, where N_t is the number of TMDs, $\omega_{tk} = 2\pi f_{tk}$ (rad/s) is the angular frequency of the kth TMD, f_{tk} (Hz) is the corresponding natural frequency of the controller, and m_{tk} (kg) and ζ_{tk} are the inertial mass and damping ratio of the kth TMD.

3. Frequency-domain procedure

A procedure to design passive inertial controllers in the frequency domain is described in this section. This approach is faced through a multi-objective optimization problem, which accounts for uncertainties associated to the modal parameters of the structure and the dynamic parameters of the human body. The H_∞ norm of the sum of closed-loop TFs of the human-structure-controller system and the cost of the controller (represented by the total inertial mass of the device) are the two objectives to be minimized. Whereas the fulfilment of the VSLS is the adopted criterion to select the solution among the optimum results generated from the optimization problem.

3.1. Optimization problem

Given the number of considered modes N_s, the number of pedestrians N_h acting on the structure, and the number of TMDs N_t, the following vectors may be defined

$$\underline{z}_s = [m_{s1}, f_{s1}, \zeta_{s1}, m_{s2}, f_{s2}, \zeta_{s2}, \ldots, m_{sN_s}, f_{sN_s}, \zeta_{sN_s}] \tag{7}$$

$$\underline{z}_s \in \mathbb{R}^+ \text{ with } [1 \times 3N_s] \text{ dimension}$$

$\underline{z}_s$ being the vector containing the parameters of the structure,

$$\underline{z}_h = [m_{h1}, f_{h1}, \zeta_{h1}, m_{h2}, f_{h2}, \zeta_{h2}, \ldots, m_{hN_h}, f_{hN_h}, \zeta_{hN_h}] \tag{8}$$

$$\underline{z}_h \in \mathbb{R}^+ \text{ with } [1 \times 3N_h] \text{ dimension}$$

$\underline{z}_h$ being the vector containing the human parameters,

$$\underline{z}_t = [m_{t1}, f_{t1}, \zeta_{t1}, m_{t2}, f_{t2}, \zeta_{t2}, \ldots, m_{tN_t}, f_{tN_t}, \zeta_{tN_t}] \tag{9}$$

$$\underline{z}_t \in \mathbb{R}^+ \text{ with } [1 \times 3N_t] \text{ dimension}$$

$\underline{z}_t$ being the vector containing the parameters of the TMDs.

Considering the aforementioned vectors, the multi-objective problem is formulated as follows

$$\min_{\underline{z}_t} \Big(J_1(\underline{z}_s, \underline{z}_h, \underline{z}_t),\ J_2(\underline{z}_t) \Big) \tag{10}$$

subjected to

$$\underline{z}_t \in [\underline{z}_{t,\min},\ \underline{z}_{t,\max}] \tag{11}$$

where J_1 and J_2 are the two objective functions, and subscripts min and max indicate the minimum and maximum values, respectively, for the search domain of $\underline{z}_t$. To account for uncertainties in the parameters of the structure and the interaction phenomenon, $\underline{z}_s$ and $\underline{z}_h$ are described by statistical distributions.

The first objective function is defined as follows

$$J_1(\underline{z}_s, \underline{z}_h, \underline{z}_t) = \max_{\omega} \sum_{p=1}^{P} \left| G_{CL}(\underline{z}_S, \underline{z}_h, \underline{z}_t, \omega) \cdot WF(\omega) \right|_p \tag{12}$$

where $p = 1, 2, \ldots\ P$, P being the number of multivariate stochastic samples generated by varying the parameters involved in the coupled system, and WF is a weighting function in the frequency domain that weighs the amplitude of G_{CL}. This function accounts for the excitability of the vibration modes of the structure depending on the harmonic of the human excitation. Note that J_1 is the H_∞ norm of a cumulative TF, which is computed by summing all the $|G_{CL}(w) \cdot WF(w)|_p$ obtained for each pth multi-variable stochastic sample.

The second objective function is expressed as follows

$$J_2(\underline{z}_t) = \sum_{k=1}^{N_t} m_{tk} \tag{13}$$

which is the total inertial mass of the vibration controllers. According to Arora [22], this mass is proportional to the manufacturing cost of the device.

Once the multi-objective optimization problem is carried out, from the set of results presented on the Pareto front, the final solution is chosen so that the VSLS is met according to the desired degree of comfort. Limits in terms of the acceleration of a structure are given in Butz et al. [7]. The criterion for that is

$$\mathrm{a}_{\mathrm{peak},95th} \leq \mathrm{a}_{lim} \tag{14}$$

being $\mathrm{a}_{\mathrm{peak},95th}$ the peak acceleration of the 95th percentile related to a certain result. Each optimal solution of the Pareto front is related to P multivariate stochastic samples. For each pth G_{CL}, the peak acceleration is computed by sweeping the input force F_a (Eq. (4)) in the frequency domain, considering that the first harmonic is between $f_{a,\min}$ and $f_{a,\max}$.

From this sweeping, the maximum acceleration is obtained as follows

$$\mathrm{a}_{\mathrm{peak}} = \max_{f_a} \left(\sum_{r=1}^{R} \left| G_{CL}(\underline{z}_s, \underline{z}_h, \underline{z}_t, r\,2\pi f_a) \right| \cdot W_h N_h \mathrm{GLF}_r \right) \tag{15}$$

$$\forall f_a \in [f_{a,\min}, f_{a,\max}]\,\mathrm{Hz}$$

then, the Cumulative Distributive Function (CDF) for the P samples is computed and the $95th$ percentile is derived, obtaining $\mathrm{a}_{\mathrm{peak},95th}$ to be applied in the selection criterion.

4. FRP footbridge

The previously explained procedure is applied to an FRP pedestrian structure, which is at design stage and is conceived following a motion-based design approach. Fig. 2 shows this design methodology, where verifications at Deflection SLS (DSLS) and Ultimate Limit State (ULS) are firstly carried out, and requirements at VSLS are secondly complied through the inclusion of vibration controllers. In this section, the FRP structure and its numerical model. As implementing a vibration control system is just justified after meeting requirements concerning static actions, results regarding this part of the design are also presented.

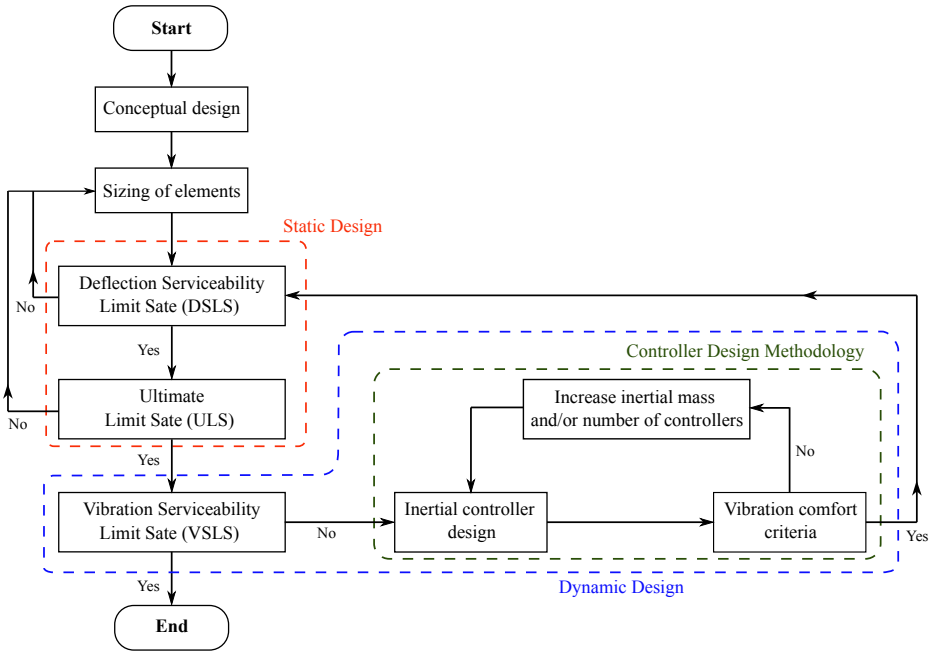

Figure 2: Motion-based design for a lively pedestrian structure.

4.1. Structure description

The subject of study is a simply supported structure, comprised of pultruded GFRP profiles and Carbon-FRP (CFRP) strips. The pedestrian structure is 10.0 m long by 1.5 m wide (Fig. 3a), and the main elements are three GFRP profiles, one I 300x150x15 and two U 300x90x15. Additionally, CFRP strips (E 139/90/4.9 and E 139/150/4.9) are bonded to the top and bottom flanges of the stringers along their entire length, as shown in Fig. 3b. GFRP I 160x80x8 elements spaced 1.25 m from the pinned supports and every 1.20 m along the rest of the bridge length are cross-beams acting as lateral restraints. Plank HD panels form the bridge deck, and a layer of recycled rubber pavement is considered as a wearing surface.

For the handrails, stainless steel cables crossing GFRP SHS 60x60x5 profiles are adopted. Stainless steel bolts class A2-50 and GFRP L 75x75x8 profiles are in charge of connecting the different FRP elements. Finally, pinned supports at the ends of each main beam are the considered elements to connect the footbridge to the concrete abutments, as presented in Fig. 3a.

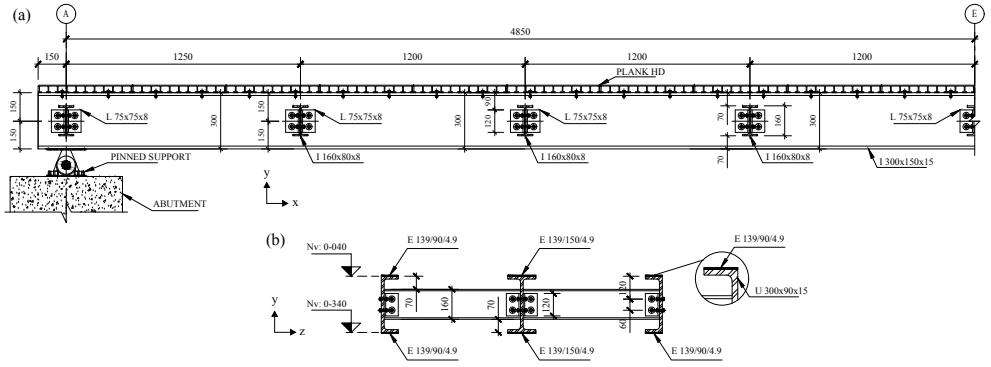

Figure 3: FRP footbridge drawings: (a) Side view , and (b) Cross-section. Dimensions in mm.

4.2. Finite Element model

Based on the previous information, a linear elastic Finite Element (FE) model of the structure is developed in ABAQUS [23], as shown in Fig. 4a. Stringers, cross-beams, handrail poles, and the deck panels are modelled with node reduced integration shell elements (S4R). Additionally, top and bottom flanges of the stringers are defined as shell composite layups composed of two plies. One layer corresponds to the GFRP laminate, and the other one refers to the CFRP strip. Mechanical properties of the employed FRP profiles are presented in the Appendix A.

To join together the stringers, cross-beams, and handrail poles, tie constraints are selected. In a similar way, connections between the stringers' top flange and the bottom part of the deck are defined. Also, 60 kg/m^2 is defined as a non-structural mass over the deck to account for the rubber pavement, L profiles, washers, nuts and bolts, which are omitted in the model. To mimic the boundary conditions of a simply supported structure assuming pinned connection mechanisms, displacements of the bottom flanges of the stringers are constrained in the longitudinal, transversal and vertical (x, y and z) directions at one end of the bridge. Whilst, only vertical (y) and transversal (z) displacements of the bottom flanges at the another end are constrained.

4.3. Static design

For the static actions, a self-weight of 0.55 kN/m^2, a non-structural load of 0.60 kN/m^2, and a uniformly distributed live load of 5.0 kN/m^2 over the bridge deck are considered as design loads. Given design guidelines do not define a clear limit for footbridges at DSLS, a long-term deflection at midspan of $L/150$ (L being the length of the span) is selected as the limit

for the pedestrian structure. Using the FE model, the deflection at midspan of the footbridge is 56 mm (L/180). Regarding the design at ULS, strength, stability, and ultimate strain checks are assumed to be satisfactory for the FRP elements. In-plane and out-of-plane failure modes of bolted connections are also considered to be verified.

4.4. Dynamic design

The dynamic response of a footbridge under the action of pedestrians can be anticipated by simple inspection of its vibration modes. Hence, a modal analysis is carried out to identify modes with natural frequencies below 10 Hz. The first two vibration modes are a flexural mode at 5.15 Hz (Fig. 4b) and a lateral-torsional mode at 6.32 Hz (Fig. 4c). These are accounted for predicting the bridge dynamic behaviour. It is worth mentioning that the third vibration mode of the footbridge is a lateral-torsional mode at 16.34 Hz, which is disregarded for the analyses since its modal contribution to the response is negligible in comparison with the contribution of the first two vibration modes. As the two shown modes display an antinodal region at midspan, the most responsive points are those located at the edges of the midspan cross-section. Hence, the inertial controller will be installed closer to this point, which from now on will be called the 'control point'.

For the VSLS assessment, two people bouncing synchronously at the control point (edge of the midspan cross-section) are considered as the design load case. Also, no other pedestrians are expected to be on the footbridge. Since bouncing can be categorized as vandalism, a minimum degree of comfort (class CL3 according to Butz et al. [7]) is chosen as the requirement to be met for this load scenario. Thus, the peak response acceleration of

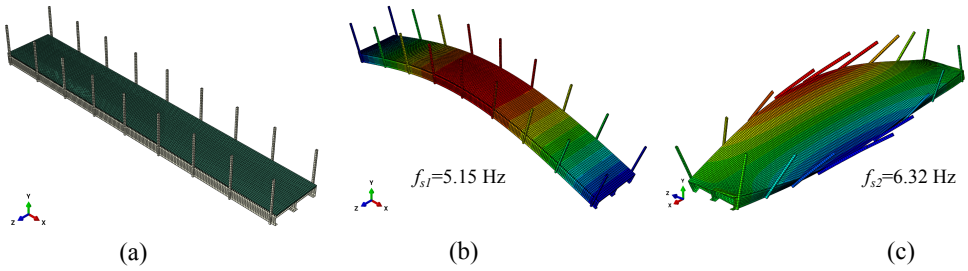

Figure 4: FE model: (a) FRP footbridge , (b) Flexural mode of vibration, and (b) Lateral-torsional mode of vibration.

the footbridge with the inertial controllers must be lower than the following limit, which is employed in Eq. (14) to select the optimal solution in the proposed frequency-domain procedure,

$$\mathrm{a}_{lim} = 2.50\,\mathrm{m/s^2}. \tag{16}$$

As bouncing can be applied directly to the control point, this harmonic loading action may be suitable to design vibration control systems for the following reasons:

- It can be maintained for a long period of time requiring low energy of the pedestrians.
- As feet remain in contact with the bridge deck, the dynamic behaviour of the structure may be actually affected by the pedestrians.
- A considerable structural resonant response may be achieved since bouncing can be applied at the most excitable location of the structure.
- The design of the controllers may be considered to be on the safety

given bouncing is a quite energetic load scenario in comparison with walking.

- As it is not a moving load, an LTI system can be adopted, enabling a fully-frequency domain analysis of the dynamic problem through a constant closed-loop TF.

5. Control design

In this section, the frequency-domain procedure explained in Section 3 is applied to design TMD systems for the FRP footbridge. To discuss the implications of HSI on the design of the controllers, the proposed approach is also applied omitting HSI.

The optimization problem, defined in Eq. (10), is used to design the controllers, which must lead to a peak response below the limit stated in Eq. (16). The following values are considered for the analyses: $N_s = 2$ vibration modes of the structure, $N_h = 2$ pedestrians bouncing synchronously, and $R = 3$ harmonics of the action. Additionally, $N_t = 1$ when a single TMD is aimed to designed, and $N_t = 2$ when the parameters of a MTMD are meant to be obtained. Considering the GLF for people bouncing proposed by Dougill et al. [14] and $\varphi_1 = \varphi_2 = \varphi_3 = 0$ rad, WF (Eq. (12)) is defined as shown in Fig. 5. Hence, 0.286, 0.095 and 0.033 are the values of the y-axis for the first, second and third harmonic, respectively. The frequency range for the harmonics, x-axis, is adopted assuming that coordinated bouncing between individuals occurs between 1 and 3 Hz [24].

Prior the solution of the optimization problem, uncertainties in the dynamic parameters of the structure and the human body are firstly described.

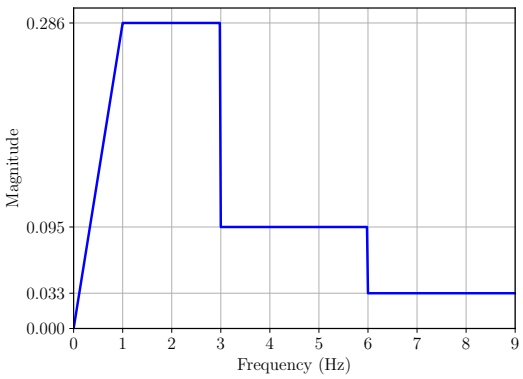

Figure 5: Weighting function.

5.1. System uncertainties

Environmental and physical conditions (e.g. temperature, moisture, mechanical cyclic loads, etc.) may influence the long-term behaviour of FRP structures during its lifespan [25]. Hence, these changes are characterized in this study by defining the parameters of the structure through statistical distributions.

To determine the statistical properties related to the effective modal mass of the flexural vibration mode, 1000 modal analysis using the FE model (Fig. 4a) are performed by only varying the non-structural mass. This parameter is assumed to follow a Normal distribution with a mean value $\mu = 60$ kg/m^2 and a Coefficient of Variation (COV) of 4% [26]. The same procedure is applied to obtain the statistical properties of the effective modal mass associated to the lateral-torsional vibration mode. The natural frequencies and damping ratios of the FRP footbridge, as stiffness and strength properties of composites, are assumed to be described by a two-parameter Weibull distribution [27]. A mean value of 5.15 Hz is assumed for the distribution of the fundamental

frequency, whereas 6.33 Hz is the mean value of the 2nd natural frequency. To account for the degradation of the structure over the years, uncertainties in the stiffness of the structural elements, flexibility of bolted connections and changes of the non-structural mass, a COV of 7% is adopted for both natural frequencies.

To complete the required data for a MSD system, a damping ratio (ζ_s) of 2% is assumed for the two vibration modes based on Hayashi et al. [28], Sobrino and Pulido [29], Stankiewicz et al. [30], and Wei et al. [31]. Additionally, a COV of 10% is adopted. Fig. 6 presents the damping ratios of 17 bridges reported in the aforementioned studies. The mean value among all the structures and the mean value suggested by the *European Guideline* [32] are also displayed in the graph.

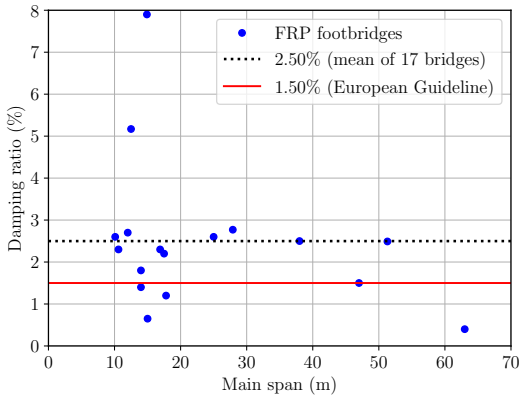

Figure 6: Damping ratios of FRP footbridges.

Uncertainties in the dynamic parameters of the human model are also considered due to the variability of values reported in literature [13]. Hence, the next considerations are adopted: (i) the mass of a person follows a Normal distribution, $\mu = 70$ kg and COV=5%, (ii) the frequency of the human

body is described by a Uniform distribution between 1.5 Hz and 6.0 Hz, and (iii) the damping ratio of a person follows a Uniform distribution between 20% and 50%. Table 1 presents the statistical properties adopted for all the described parameters. Assuming that all the statistical distributions of the structure and the human body are mutually independent, 500, 1000, 2500, and 5000 stochastic samples (P) are generated using the Latin Hypercube (LH) method. Since the $a_{peak,95th}$ (Eq. (15)) of the uncontrolled coupled systems does not vary significantly after 1000 multivariate samples, this number of human-structure systems is selected for the design of the controllers.

Table 1: Characterization of the dynamic parameters of the FRP footbridge and the human body

Parameter	Description	Units	Statistical properties		
			Distribution	μ/σ	Range
m_{s1}	Eff. modal mass, mode 1	kg	Normal	834.6/17.6	-
m_{s2}	Eff. modal mass, mode 2	kg	Normal	451.4/7.3	-
f_{s1}	Natural frequency, mode 1	Hz	Weibull	5.15/0.36	-
f_{s2}	Natural frequency, mode 2	Hz	Weibull	6.32/0.44	-
ζ_{s1}, ζ_{s2}	Damping ratio, 2 modes	%	Weibull	2/0.02	-
m_h	Mass	kg	Normal	70.0/4.0	-
f_h	Natural frequency	Hz	Uniform	-	1.5 - 6.0
ζ_h	Damping ratio	%	Uniform	-	20 - 50

5.2. Designed controllers

Among the several metaheuristic techniques currently available, the Genetic Algorithm (GA) has proved to be a power tool to solve engineering problems [33]. Hence, a multi-objective controlled elitist GA, provided by a toolbox of MATLAB [34], is employed. For all the scenarios, an initial population of 100 individuals is defined, and the maximum number of iterations is set to 100. The search domain for the mass, frequency and damping ratio of the controllers ($\underline{z}_t$) depending on the scenario are presented in Table 2.

Table 2: Search domain for parameters of the controllers

Interaction	System	Parameter	Unit	Domain
No HSI	TMD	m_t	kg	$[0-160]$
		f_t	Hz	$[4.6-7.6]$
		ζ_t	%	$[2-22]$
	MTMD	m_{tk}	kg	$[0-80]$
		f_{tk}	Hz	$[4.6-7.6]$
		ζ_{tk}	%	$[2-22]$
With HSI	TMD	m_t	kg	$[0-60]$
		f_t	Hz	$[4.6-7.6]$
		ζ_t	%	$[2-12]$
	MTMD	m_{tk}	kg	$[0-30]$
		f_{tk}	Hz	$[4.6-7.6]$
		ζ_{tk}	%	$[2-12]$

Fig. 7 displays the Pareto Fronts obtained after carrying out the optimization, neglecting and considering HSI in the analyses, to design a TMD

and a MTMD. Whilst in Table 3, the controllers selected from the set of optimum solutions according to the criterion presented in Eq. (14) are shown. The number associated to each TMD or MTMD indicates the total inertial mass of the device. Note that the designed parameters of the controllers are not practical when HSI is neglected, especially the value of ζ_t. Despite the high values of the parameters for the TMD (m_t and ζ_t), the desired degree of comfort is not even achieved ($a_{peak,95th} = 2.58$ m/s^2).

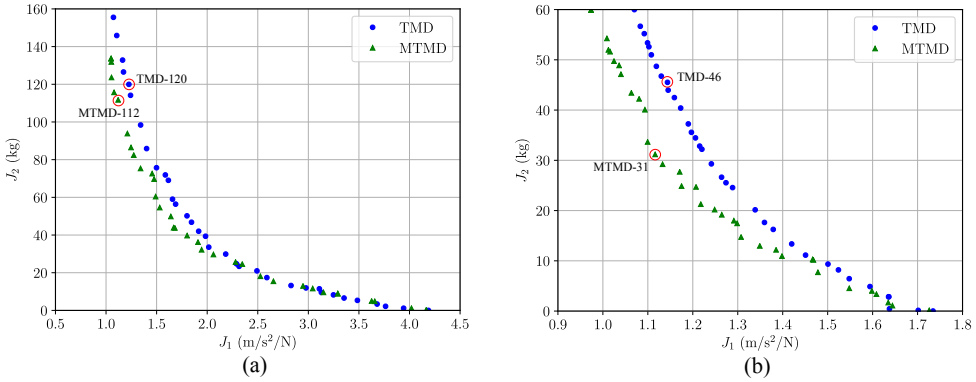

Figure 7: Pareto front to design controllers: (a) Omitting HSI, and (b) Considering HSI.

Due to the inclusion of HSI, the maximum acceleration at the 95th percentile of the uncontrolled systems is significantly reduced, from 12.24 m/s^2 to 3.81 m/s^2. In addition, both control systems, the TMD and the MTMD, allow to meet the requirement at VSLS when the interaction phenomenon is taken into account. A reduction of 35% of the $a_{peak,95th}$ (from 3.81 m/s^2 to 2.49 m/s^2) is reached for the two control systems. Given the TMD-46 presents a larger inertial mass than the MTMD-31, the latter may be considered as a better option due to the lower value of J_2. This shows the importance of the second controller to increase the frequency band of effectiveness in the

Table 3: Design of the controllers for 2 people bouncing

Interaction	System	Designed parameters	J_1 (m/s^2/N)	J_2 (kg)	$a_{peak,95th}$ (m/s^2)
No HSI	Uncontrolled	-	4.20	-	12.24
	TMD-120	$m_t = 120.0$ kg	1.23	120.0	2.58
		$f_t = 4.56$ Hz			
		$\zeta_t = 20.5\%$			
	MTMD-112	$m_{t1} = 72.1$ kg, $m_{t2} = 39.6$ kg	1.11	111.7	2.49
		$f_{t1} = 4.24$ Hz, $f_{t2} = 5.35$ Hz			
		$\zeta_{t1} = 16.2\%$, $\zeta_{t2} = 14.4\%$			
With HSI	Uncontrolled	-	1.74	-	3.81
	TMD-46	$m_t = 45.5$ kg	1.14	45.5	2.49
		$f_t = 4.92$ Hz			
		$\zeta_t = 10.9\%$			
	MTMD-31	$m_{t1} = 27.2$ kg, $m_{t2} = 4.0$ kg	1.12	31.2	2.49
		$f_{t1} = 4.76$ Hz, $f_{t2} = 5.82$ Hz			
		$\zeta_{t1} = 10.4\%$, $\zeta_{t2} = 2.7\%$			

MTMD system. Note that the second TMD, which is only 4 kg, allows to reduce the total inertial mass of the first controller from 45.5 kg to 27.2 kg.

Accounting for Fig. 2 and assuming that the MTMD-31 is installed once the footbridge is built, DSLS and ULS checks are carried out again. Thus, the computed long-term deflection using the FE model is 57 mm ($L/175$), and it is considered that the requirements at ULS are also met to complete the structural design of the FRP footbridge.

5.3. Control performance

The CDF curves of the H_∞ norm related to each pth multivariate stochastic sample are employed to quantify the reduction of vibration that the controllers provide. This reduction is calculated from the total area between the CDF curve and the y-axis, so a single value can be obtained as follows

$$\text{Reduction}_{\text{CDF}} = \frac{\text{Uncontrolled CDF}_{\text{area}} - \text{Controlled CDF}_{\text{area}}}{\text{Uncontrolled CDF}_{\text{area}}}. \tag{17}$$

To compare the performance of the controllers, devices with similar mass are selected from the Pareto fronts presented in Fig. 7b. Fig. 8 displays a comparison of the cumulative function of $|G_{CL}(\underline{z}_S, \underline{z}_h, \underline{z}_t, \omega) \cdot WF(\omega)|_p$ and the corresponding CDF curves of the H_∞ norm (peak value of the frequency weighted closed-loop TF) for the chosen controllers. Whereas in Table 4, the reduction obtained from the CDF curves together with the achieved $\text{a}_{\text{peak},95th}$ of different systems considering HSI are presented.

If controllers with a mass around 31 kg are compared, the comfort level is not met with the inclusion of a single TMD. Therefore, this solution would not be suitable to comply the design requirement at VSLS. When a TMD or a MTMD with mass values of 46 kg approximately are employed, the comfort level is reached by both, but the latter outperforms the former. For the same peak response at the 95th percentile, the TMD-46 and the MTMD-31 seem to perform almost identical. Nevertheless, the mass value of the TMD-46 is 31% larger than value of the MTMD-31.

5.4. Control design with a classical approach

Different procedures can be adopted to design passive inertial controllers for pedestrian structures, especially for a single TMD. Thus, a comparison

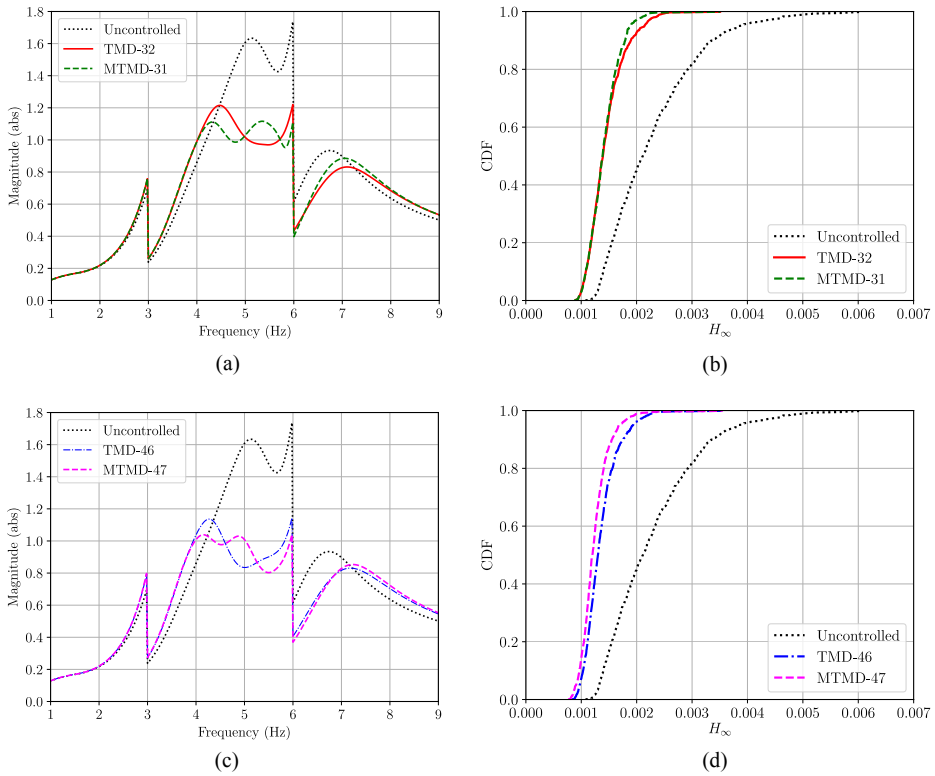

Figure 8: Performance of controllers with similar mass: (a) Cumulative function, 31 kg, (b) CDF of H_∞, 31 kg, (c) Cumulative function, 46 kg, and (d) CDF of H_∞, 46 kg.

of results is presented herein when the parameters of a vibration control device are obtained employing deterministic analytical expressions. Regarding the design of a MTMD, no comparison is presented given well-established procedures are not available in existing design guidelines.

To design optimally a TMD, Boniface et al. [6] or Butz et al. [7] still recommend design principles from the theoretical approaches carried out by Den Hartog [35]. For an undamped system excited by a harmonic load, this pioneering study considers that the optimal frequency ($f_{t,DH}$) and damping ratio ($\zeta_{t,DH}$) of a TMD may be obtained as follows

Table 4: Reduction of vibration considering HSI

System	Mass (kg)	$\text{Reduction}_{\text{CDF}}$ (%)	$a_{\text{peak},95th}$ (m/s^2)	Comfort level
TMD-32	32.2	36	2.61	CL4
MTMD-31	31.2	38	2.49	CL3
TMD-46	45.5	40	2.49	CL3
MTMD-47	47.1	46	2.40	CL3

$$f_{t,DH} = \frac{1}{1+\mu_t} f_s \tag{18}$$

$$\zeta_{t,DH} = \sqrt{\frac{3\mu_t}{8(1+\mu_t)}} \tag{19}$$

where μ_t is the ratio between the TMD's inertial mass and the effective modal mass of the vibration mode to be controlled (m_t/m_s).

As specific values of μ_t and f_s should be firstly adopted to design the TMD, the following values are considered: $m_s = 834.6$ kg (Table 1), $f_s = 5.15$ Hz (Fig. 4), and $m_t = 45.5$ kg (Table 3). Employing Eqs. (18)-(19), the parameters obtained are $f_{t,DH} = 4.88$ Hz and $\zeta_{t,DH} = 13.9\%$. Since the traditional approaches do not consider HSI, the performance of the designed device is firstly evaluated omitting the interaction phenomenon. Hence, only the 1000 systems of the structure are employed. Secondly, the analyses are carried out including HSI, so the stochastic human-structure systems are considered. Table 5 presents the reduction of the response using Eq. (17) and the $a_{\text{peak},95th}$ for both scenarios together with the results of the proposed

procedure.

Table 5: Designed parameters for a TMD with a moving mass (m_t) of 45.5 kg

Approach	$\text{Reduction}_{\text{CDF}}$ (%)	$\text{a}_{\text{peak},95th}$ (m/s^2)
Den Hartog without HSI	74	3.73
Den Hartog with HSI	40	2.50
Proposed procedure	40	2.49

Although similar f_t and ζ_t are determined using the classical approach and the proposal of this paper, the achieved $\text{a}_{\text{peak},95th}$ differ vastly when HSI is neglected. An overestimation of the bridge response is calculated even if the TMD is modelled with the system of the structure, as discussed in Sec-tion 5.2. The reduction of 74% seems to be significant for this scenario, but this is explained by the fact that the responses of the uncontrolled structures are also large. When HSI is considered to evaluate the performance of the TMD designed through the approach Den Hartog [35], results are quite sim-ilar to those obtained following the proposed procedure. The importance of accounting for HSI is once again highlighted by this result, demonstrating the benefit of considering a coupled human-structure-controller system in the dynamic analysis of a lightweight pedestrian structure.

6. Time history results

In this section, time history results considering two pedestrians actions are presented to validate the proposed frequency-domain approach and further

compare the performance of the designed controllers. First, results computed through the FE model, described in Section 4.2, are compared with values obtained from the G_{CL} model (Section 2.1) when two people bounce on the uncontrolled structure. For these analyses, it is assumed that the second harmonic of bouncing is synchronized with the fundamental frequency of the structure. Second, the response reduction due to the controllers is assessed when a single pedestrian crosses the FRP footbridge. Different gait frequencies (f_a) are studied for this load scenario, considering that a vibration mode of the structure is excited in resonance by one of the harmonics of a walking pedestrian.

6.1. Bouncing action

For the analysis carried out in ABAQUS [23], each pedestrian is represented by a MSD system plus an external harmonic force (F_{ha}), as shown in Fig. 9a. To define F_{ha}, which only affects the structure, Eq. (4) can be used, but coefficients referred as Vertical Dynamic Load Factors (VDLFs) are employed instead of the GLFs. If certain coefficients are known, the others can be computes since they are related through the following expression

$$\mathrm{VDLF}_r = \mathrm{GLF}_r \cdot \left|G_H(s)\right|_{s=j2\pi f_a}. \tag{20}$$

Two MSD systems located near the edge of the midspan section are considered in the FE model (Fig. 9a), and the corresponding harmonic forces of each human are applied at the deck nodes. To represent a person bouncing, the following values are adopted: $m_h = 66$ kg, $f_h = 2.30$ Hz, $\zeta_h = 25\%$, GLF_1 =0.286, GLF_2 =0.095, and GLF_3 =0.033 [14]. Hence, $\mathrm{VDLF}_1 = 0.582$,

$\mathrm{VDLF}_2 = 0.114$, and $\mathrm{VDLF}_3 = 0.036$ are used to describe the external harmonic force in the FE model.

In ABAQUS, HSI is achieved by means of contact between the bottom node of the MSD system and the deck surface. The footbridge, pedestrians, harmonic loads, and the interaction phenomenon lead to a nonlinear coupled system, which global system of equations may be expressed by the following matrix form

$$\begin{bmatrix} \boldsymbol{M_h} & \boldsymbol{0} \\ \boldsymbol{0} & \boldsymbol{M_s} \end{bmatrix} \begin{Bmatrix} \ddot{\boldsymbol{y}}_{\boldsymbol{h}} \\ \ddot{\boldsymbol{y}}_{\boldsymbol{s}} \end{Bmatrix} + \begin{bmatrix} \boldsymbol{C_h} & \boldsymbol{0} \\ \boldsymbol{0} & \boldsymbol{C_s} \end{bmatrix} \begin{Bmatrix} \dot{\boldsymbol{y}}_{\boldsymbol{h}} \\ \dot{\boldsymbol{y}}_{\boldsymbol{s}} \end{Bmatrix} + \cdots \\ \cdots \begin{bmatrix} \boldsymbol{K_h} & \boldsymbol{0} \\ \boldsymbol{0} & \boldsymbol{K_s} \end{bmatrix} \begin{Bmatrix} \boldsymbol{y_h} \\ \boldsymbol{y_s} \end{Bmatrix} = \begin{Bmatrix} \boldsymbol{F_{ha}} \\ \boldsymbol{0} \end{Bmatrix} + \begin{Bmatrix} \boldsymbol{F_h^c} \\ \boldsymbol{F_s^c} \end{Bmatrix} \tag{21}$$

where $\boldsymbol{M_h}$, $\boldsymbol{C_h}$ and $\boldsymbol{K_h}$ are the mass, damping and stiffness matrices of the human system, $\boldsymbol{M_s}$, $\boldsymbol{C_s}$ and $\boldsymbol{K_s}$ are the mass, damping and stiffness matrices of the footbridge, $\boldsymbol{F_{ha}}$ is the external harmonic force vector of the pedestrian, $\boldsymbol{F_h^c}$ is the force vector applied on the human as consequence of the interaction with structure, and $\boldsymbol{F_s^c}$ represents its counterpart on the footbridge, $\ddot{\boldsymbol{y}}_{\boldsymbol{h}}$ and $\ddot{\boldsymbol{y}}_{\boldsymbol{s}}$ are the acceleration response vectors, $\dot{\boldsymbol{y}}_{\boldsymbol{h}}$ and $\dot{\boldsymbol{y}}_{\boldsymbol{s}}$ are the velocity response vectors, and $\boldsymbol{y_h}$ and $\boldsymbol{y_s}$ are the displacement response vectors of the pedestrian and bridge, respectively. To solve the system of differential equations shown in Eq. (21), HHT-α implicit integration method is employed. Also, a constant time step of 0.001 s and Rayleigh damping of 2% are adopted for the calculation, and the structural is computed at the edge of the midspan section when the two pedestrians bounce for 5 s.

For comparison, the response of the uncontrolled structure is obtained

by implementing the block diagram shown in Fig. 1b in SIMULINK [34]. Two vibration modes ($N_s = 2$) of the structure are assumed to be excited by two pedestrians ($N_h = 2$), and no controllers are considered. The fourth-order Runge-Kutta formula is adopted as the solver method with a time step of 0.001 s. The results employing the FE model and this approach are displayed in Fig. 9b. It can be seen that the maximum response is quite similar using ABAQUS (2.76 m/s^2) and SIMULINK (2.83 m/s^2). The peak acceleration (2.91 m/s^2) obtained from Eq. (15) is also displayed in the graph with a dash line, demonstrating that the proposed frequency-domain approach allows to simplify the analysis without excessive loss of accuracy. In contrast to the approaches using the FE model and the block diagram, the proposal of this paper only requires the computation of algebraic operations to obtain the peak of the steady-state response of a structure subjected to bouncing pedestrians. Hence, the proposed procedure is suitable for carrying out analyses including uncertainties.

6.2. Walking action

To represent a pedestrian crossing the FRP footbridge, a MSDA system moving with a certain velocity, v (m/s), over a simply supported beam is considered herein. In Fig. 10a, the case when the structure incorporates a single TMD while accounting for the walking person is displayed. The block diagram for this load scenario is represented in Fig. 10b, where the same TFs defined in Section 2 are employed. As the system that represents the person modifies its location, y (m), the mode shape (ϕ) of the analysed vibration mode should be additionally included in the diagram. This allows to consider the interaction of the MSDA system with the structure at different instants.

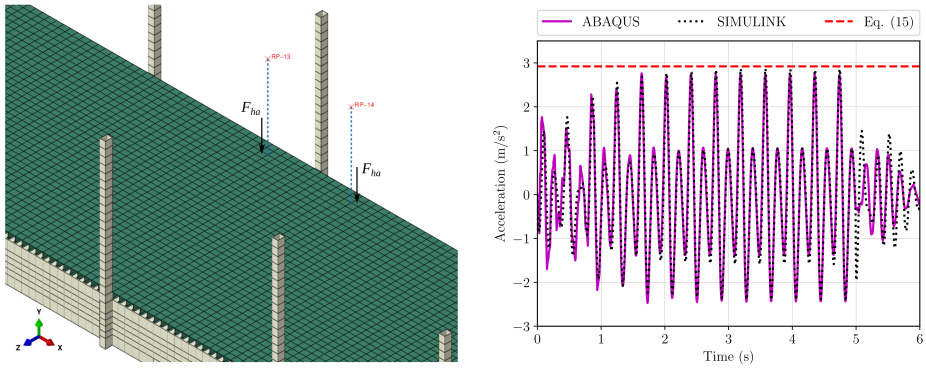

(a) (b)

Figure 9: Comparison of results for the uncontrolled FRP footbridge with two people bouncing: (a) MSD systems in the FE model, and (b) Vertical acceleration at the edge of the midspan cross-section.

Since the dynamic parameters of the human body and the pedestrian force change according to the performed action, the HSI model of a walking pedestrian reported by [36] is employed. The values considered for the human system are: $m_h = 60.6$ kg (86% of 70 kg), $f_h = 2.96$ Hz, $\zeta_h = 46\%$, $\text{VDLF}_1 = 0.273$, and VDLF_2=0.047. To account for a third harmonic of the action VDLF_3=0.024 is assumed considering that ISO [8] states $\text{DLF}_3 \simeq \text{DLF}_2/2$ for walking. Therefore, GLF_1 =0.303, GLF_2 =0.040, and GLF_3 =0.022 are the computed coefficients to define F_a from Eq. (20).

Considering that a person crosses the bridge on a lane near to one of the edges, it is assumed that two vibration modes of the FRP footbridge are excited, $N_s = 2$ in Eq. (2). As considered in other studies [37, 38] and based on the modal amplitudes (normalized to the maximum displacement) extracted from ABAQUS (Fig. 4), the following expression is adopted to

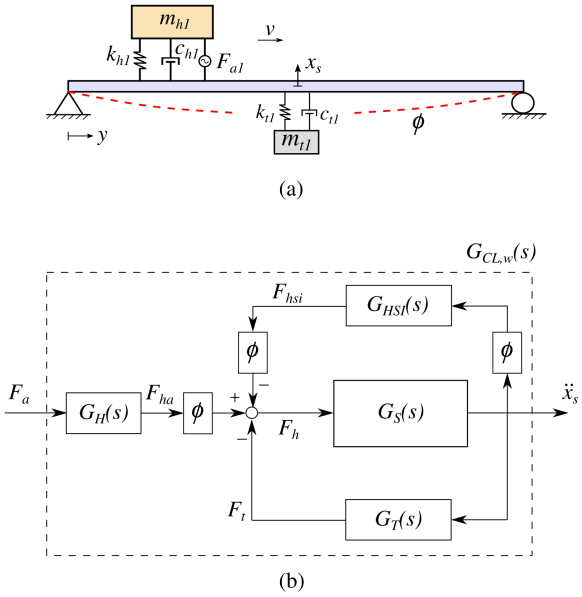

Figure 10: Pedestrian walking: (a) Schematic representation, and (b) Block diagram.

define analytically the mode shape of both vibration modes

$$\phi = \sin\left(\frac{\pi y}{L}\right). \tag{22}$$

Hence, Eq. (22) describes the mode shape in the vertical direction of the Mode 1 (flexural vertical mode) and the Mode 2 (lateral-torsional mode). For the dynamic analysis, the block diagram shown in Fig. 10b is implemented in SIMULINK [34] considering two vibration modes, and the Runge-Kutta formula is adopted again as the solver method with a time step of 0.001 s.

The performance of the TMD-46 and the MTMD-31 considering uncertainties is assessed with the same 1000 systems of the structure generated in Section 5.1. Whereas to define the walking pedestrian, a Normal distribution, $\mu = 70$ kg and COV=5%, is adopted for m_h, and a Uniform distribution between 10% and 60% is assumed for ζ_h. Regarding f_h, its value is taken

equal to the gait frequency of the resonant harmonic, $f_h = f_a = f_s/r$ [39, 40]. Considering the mentioned distributions, 1000 stochastic systems are generated using the LH method to represent the walking person. Additionally, $v = 1.70$ m/s is adopted as the velocity of the pedestrian to cross the FRP footbridge in all cases [41].

Assuming that a harmonic of the human action excites a certain vibration mode of the structure, two scenarios are investigated. First, the pedestrian third harmonic is considered to be synchronized with the second natural frequency of the footbridge ($f_a = f_{s2}/3$). Accounting for the nominal values to describe the footbridge (Table 1) and the walker [36], Figs. 11a and c show the time history response of the structure at midspan with the TMD-31 and the MTMD-46, respectively. Second, the Mode 1 of the structure is assumed to be always excited by the second harmonic of the person ($f_a = f_{s1}/2$). In Figs. 11b and d, the footbridge vibration levels at midspan with the TMD-46 and the MTMD-31, respectively, are displayed. In the fourth cases, a reduction of the acceleration is appreciated due to the designed controllers, but the single device shows a slightly better performance than the MTMD-31. This may be explained by the fact that the TMD-46 affects the two vibration modes of the structure as their natural frequencies ($f_{s1} = 5.15$ Hz and $f_{s2} = 6.32$ Hz) are close.

The CDF curves of the maximum acceleration (a_{max}) computed in each one of the 1000 analyses is shown in Figs. 11e-f for both scenarios of the resonant harmonics. From these curves, the TMD-46 seems to control slightly better than the MTMD-31 the human-induced vibrations, especially for the case of the second harmonic ($r = 2$) exciting the Mode 1. This is expected

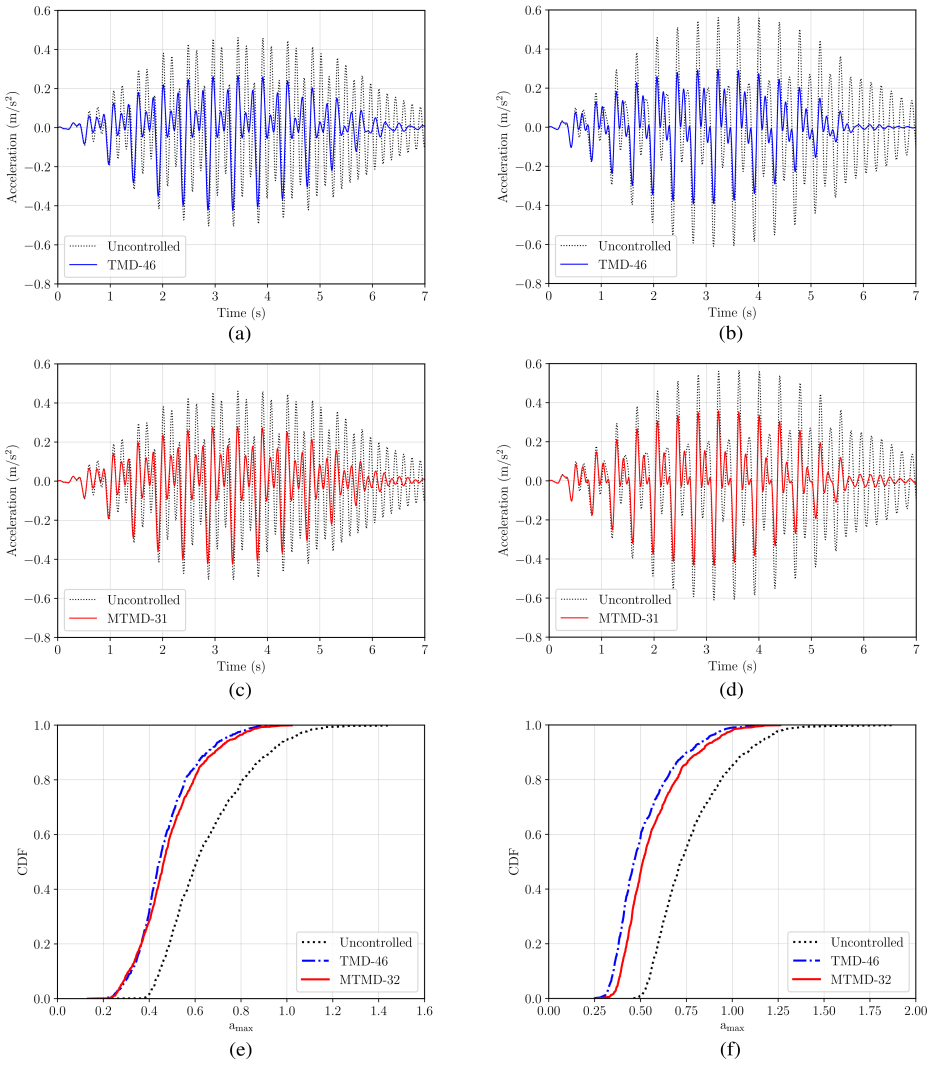

Figure 11: Acceleration response at midspan due to a walking pedestrian: (a) Structure+TMD when $f_a = f_{s2}/3$, (b) Structure+TMD when $f_a = f_{s1}/2$, (c) Structure+MTMD when $f_a = f_{s2}/3$, (d) Structure+MTMD when $f_a = f_{s1}/2$, (e) CDF when $f_a = f_{s2}/3$, and (f) CDF when $f_a = f_{s1}/2$.

since the mass of the TMD-46 (45.5 kg) is 40% larger than the mass of the first controller (27.2 kg) of the MTMD-31. When the third harmonic ($r = 3$)

of the person is synchronized with f_{s2}, both designed controller show a similar performance. However, the MTMD is a better alternative as its total inertial mass (31.2 kg) is significantly lower than the one of TMD.

Using Eq. (17), the reduction of the response due to the TMD-46 and the MTMD-31 is assessed considering the CDF curves. These results together with the maximum acceleration at the 95th percentile ($a_{max,95th}$) are presented in Table 6. Both vibration control systems lead to a medium comfort level, CL2 ($0.50 \leq a_{max} < 1.00$ m/s^2), when a pedestrian crosses the structure synchronizing one of his/her harmonics with the natural frequency of a certain vibration mode of the structure. Designing controllers in the frequency domain accounting for bouncing, which allows to work with a LTI system, may be practical and fast, especially when uncertainties associated to the structure and HSI are considered. Then, an adequate behaviour of a lively footbridge under other human activities (e.g. walking or running) can be checked.

Table 6: Reduction of vibration considering a walking pedestrian

System	Third harmonic, $f_a = f_{s2}/3$			Second harmonic, $f_a = f_{s1}/2$		
	$\text{Reduction}_{\text{CDF}}$ (%)	$a_{max,95th}$ (m/s^2)	Comfort Level	$\text{Reduction}_{\text{CDF}}$ (%)	$a_{max,95th}$ (m/s^2)	Comfort Level
Uncontrolled	-	1.01	CL3	-	1.18	CL3
TMD-46	28	0.73	CL2	34	0.86	CL2
MTMD-31	26	0.77	CL2	27	0.92	CL2

Considering the TMD designed through the approach of Den Hartog [35],

the midspan response of FRP footbridge with the controller is also assessed under the action a single pedestrian. Table 7 presents the results of this load scenario. Similarly to the bouncing load case, an overestimation of the response of the bridge-TMD system is obtained when HSI is neglected, regardless the gait frequency. In fact, a worse comfort level is obtained. When the interaction phenomenon is considered, similar $a_{max,95th}$ and CL are obtained employing the classical approach and the proposed methodology. This expected as the parameters of the TMD presented in Sections 5.2 and 5.4 are almost identical.

Table 7: Comparison of results for the FRP footbridge with the TMD-46 subjected to a walking pedestrian

Approach	Third harmonic, $f_a = f_{s2}/3$		Second harmonic, $f_a = f_{s1}/2$	
	$a_{max,95th}$ (m/s^2)	Comfort Level	$a_{max,95th}$ (m/s^2)	Comfort Level
Den Hartog without HSI	1.54	CL3	1.61	CL3
Den Hartog with HSI	0.72	CL2	0.88	CL2
Proposed procedure	0.73	CL2	0.86	CL2

7. Conclusions

A frequency-domain framework has been proposed for the robust design of vibration control devices in lightweight pedestrian structures susceptible to interaction phenomenon. Although several sophisticated models to account for HSI are available nowadays, this paper takes advantage of a fairly simple

human-structure-controller system to tackle the dynamic problem through a closed-loop TF, which allows to model efficiently HSI on lightweight structures subjected to harmonic loads.

By including uncertainties from the dynamic parameters of the structure and the pedestrians, a TMD and a MTMD have been designed for a 10-m long FRP footbridge. The inclusion of these control systems to mitigate the excessive human-induced vibrations has been studied in the frequency and time domains, demonstrating an enhancement of the dynamic behavior of the structure at VSLS. Accounting for the obtained results, the following conclusions may be drafted:

- An over dimensioning of passive inertial controllers could be obtained by omitting HSI.
- The inclusion of a MTMD leads to a less sensitive to uncertainties and lighter control system in comparison with a single TMD.
- For the same total mass, a MTMD is more effective than a single TMD to mitigate multi-harmonic structural responses. Thus, several TMDs can be distributed along a frequency band to provide more robustness in the structural performance of a lightweight footbridge.
- In contrast with an analysis using a FE model, the proposed frequency-domain approach allows to simplify the computation of the peak response of a structure subjected to pedestrians bouncing. Thus, the proposal is suitable to carry out analyses including uncertainties due to its computational efficiency.

Finally, it is important to mention that the proposed methodology to design passive inertial controllers is general and suitable to other pedestrian structures regardless the material used to build the footbridge. As the proposal employs SDOF systems to represent the vibration modes of a footbridge, only the statistical properties associated to the modal parameters should be modified according to the inherent characteristics of the construction material. Moreover, this procedure is can be applied to other types of inertial controller (including semi-active and active TMDs) just by changing the control parameters. In the future, representing a crowd of walking pedestrians through a LTI system, similarly to the coupled human-structure system with bouncing people, will be investigated to further develop the frequency-domain proposal of this work.

CRediT authorship contribution statement

Christian Gallegos-Calderón: Conceptualization, Methodology, Software, Validation, Formal analysis, Investigation, Data curation, Writing – original draft, Visualization. **Carlos M. C. Renedo**: Methodology, Software, Validation, Formal analysis, Investigation, Data curation, Writing – original draft, Visualization. **M. Dolores G. Pulido**: Methodology, Resources, Supervision, Writing – re-view & editing. **Iván M. Díaz**: Conceptualization, Methodology, Resources, Supervision, Writing – re-view & editing, Project administration, Funding acquisition.

Acknowledgments

The authors acknowledge the grant RTI2018-099639-B-I00,'Structural efficiency enhancement for bridges subjected to dynamic loading: integrated

smart damper', funded by MCIN/AEI/10.13039/501100011033 and by 'ERDF A way of making Europe'. Christian Gallegos-Calderón expresses his gratitude to the Secretariat of Higher Education, Science, Technology and Innovation of Ecuador (SENESCYT) for the scholarship CZ02-000167-2018.

References

[1] P. Dey, S. Walbridge, S. Narasimhan, Vibration Serviceability Analysis of Aluminum Pedestrian Bridges Subjected to Crowd Loading, in: 6th International Conference on Advances in Experimental Structural Engineering, Urbana-Champaign, USA, 2015.

[2] E. Ahmadi, C. Caprani, S. Živanović, A. Heidarpour, Vertical ground reaction forces on rigid and vibrating surfaces for vibration serviceability assessment of structures, Engineering Structures 172 (2018) 723–738.

[3] J. Russell, X. Wei, S. Živanović, C. Kruger, Vibration serviceability of a GFRP railway crossing due to pedestrians and train excitation, Engineering Structures 219 (2020) 110756.

[4] S. Živanović, G. Feltrin, J. T. Mottram, J. M. Brownjohn, Vibration performance of bridges made of fibre reinforced polymer, in: Conference Proceedings of the Society for Experimental Mechanics Series, volume 4, Orlando, FL, 2014, pp. 155–162.

[5] E. Shahabpoor, A. Pavic, V. Racic, Interaction between Walking Humans and Structures in Vertical Direction: A Literature Review, Shock and Vibration 2016 (2016) 1–22.

[6] V. Boniface, V. Bui, P. Bressolette, P. Charles, X. Cespedes, Footbridges: Assessment of vibrational behaviour of footbridges under pedestrian loading, Service d'Études Techniques des Routes et Autoroutes, Paris, 2006.

[7] C. Butz, C. Heinemeyer, A. Keil, M. Schlaich, A. Goldack, S. Trometer, M. Lukić, B. Chabrolin, A. Lemaire, P.-O. Martin, Á. Cunha, E. Caetano, HIVOSS: Design of footbridges guideline, Research Fund for Coal and Steel, 2008.

[8] ISO, ISO 10137 - Bases for design of structures - Serviceability of buildings and walkways against vibrations, volume 10137, International Organization for Standardization, 2007.

[9] F. T. Silva, H. M. B. F. Brito, R. L. Pimentel, Modeling of crowd load in vertical direction using biodynamic model for pedestrians crossing footbridges, Canadian Journal of Civil Engineering 40 (2013) 1196–1204.

[10] E. Shahabpoor, A. Pavic, V. Racic, Identification of mass-spring-damper model of walking humans, Structures 5 (2016) 233–246. doi:10.1016/j.istruc.2015.12.001.

[11] Q. Zhu, W. Yang, Y. Du, S. Živanović, Investigation of a vibration mitigation method based on crowd flow control on a footbridge, Structures 33 (2021) 1495–1509. doi:10.1016/j.istruc.2021.05.034.

[12] J. W. Qin, S. S. Law, Q. S. Yang, N. Yang, Finite element analysis of

pedestrian-bridge dynamic interaction, Journal of Applied Mechanics, Transactions ASME 81 (2014).

[13] C. A. Jones, P. Reynolds, A. Pavic, Vibration serviceability of stadia structures subjected to dynamic crowd loads: A literature review, Sound and Vibration 330 (2011) 1531–1566.

[14] J. W. Dougill, J. R. Wright, J. G. Parkhouse, R. E. Harrison, Human structure interaction during rhythmic bobbing, The Structural Engineer (2006) 32–39.

[15] C. M. Renedo, I. M. Díaz, J. M. Russell, S. Živanovic, Performance of inertial mass controllers for ultra-lightweight footbridges: A case study, in: xi International Conference on Structural Dynamics EURODYN, volume 1, Athens, Greece, 2020, pp. 1741–1746.

[16] J. M. Soria, I. M. Díaz, J. H. García-Palacios, Further steps towards the tuning of inertial controllers for broadband-frequency-varying structures, Structural Control and Health Monitoring 27 (2020).

[17] E. Caetano, Á. Cunha, C. Moutinho, F. Magalhães, Studies for controlling human-induced vibration of the Pedro e Inês footbridge, Portugal. Part 2: Implementation of tuned mass dampers, Engineering Structures 32 (2010) 1082–1091.

[18] L. Wang, W. Shi, Q. Zhang, Y. Zhou, Study on adaptive-passive multiple tuned mass damper with variable mass for a large-span floor structure, Engineering Structures 209 (2020) 110010.

[19] W. D. Varela, R. C. Battista, Control of vibrations induced by people walking on large span composite floor decks, Engineering Structures 33 (2011) 2485–2494.

[20] K. Van Nimmen, P. Verbeke, G. Lombaert, G. De Roeck, P. Van den Broeck, Numerical and Experimental Evaluation of the Dynamic Performance of a Footbridge with Tuned Mass Dampers, Journal of Bridge Engineering 21 (2016) C4016001.

[21] N. Garcia-Troncoso, A. Ruiz-Teran, P. J. Stafford, Attenuation of pedestrian-induced vibrations in girder footbridges using tuned-mass dampers, Advances in Bridge Engineering 1 (2020) 1–26.

[22] J. S. Arora, Optimization of structural and mechanical systems, World Scientific Publishing Co., 2007.

[23] SIMULIA, Abaqus 2020 Analysis User's Guide, Dassault Systèmes Simulia Corporation, 2020.

[24] E. Duarte, T. Ji, Action of Individual Bouncing on Structures, Journal of Structural Engineering 135 (2009) 818–827.

[25] T. Stratford, The condition of the Aberfeldy Footbridge after 20 years in service, in: Structural Faults and Repair, Edinburgh, UK, 2012.

[26] JCSS, JCSS Probabilistic Model Code, 2001.

[27] M. Alqam, R. M. Bennett, A. H. Zureick, Three-parameter vs. two-parameter Weibull distribution for pultruded composite material properties, Composite Structures 58 (2002) 497–503.

[28] G. Hayashi, C. W. Kim, Y. Suzuki, K. Sugiura, P. J. McGetrick, H. Hibi, Monitoring and model updating of an FRP pedestrian truss bridge, in: 5th International Symposium on Life-Cycle Engineering, IALCCE 2016, Delft, 2017, pp. 756–763.

[29] J. A. Sobrino, M. D. G. Pulido, Towards advanced composite material footbridges, Structural Engineering International: Journal of the International Association for Bridge and Structural Engineering (IABSE) 12 (2002) 84–86.

[30] B. Stankiewicz, P. Górski, M. Tatara, All-GFRP footbridge under human-induced excitation, MATEC Web of Conferences 262 (2019) 10013.

[31] X. Wei, J. Russell, S. Živanović, J. Toby Mottram, Measured Dynamic Properties for FRP Footbridges and their Critical Comparison against Structures Made of Conventional Construction Materials, Composite Structures (2019) 110956.

[32] JRC, Prospect for New Guidance in the Design of FRP, European Commission, Joint Research Centre, 2016.

[33] J. Nocedal, S. Wright, Numerical Optimization, Springer Series in Operations Research and Financial Engineering, Springer New York, 2006.

[34] Mathworks, MATLAB - Getting Started Guide, Matick, 2019.

[35] J. P. Den Hartog, Mechanical vibrations, McGraw-Hill Book Company, New York, 1934.

[36] J. F. Jiménez-Alonso, A. Sáez, E. Caetano, F. Magalhães, Vertical Crowd-Structure Interaction Model to Analyze the Change of the Modal Properties of a Footbridge, Journal of Bridge Engineering 21 (2016).

[37] L. Wang, S. Nagarajaiah, W. Shi, Y. Zhou, Semi-active control of walking-induced vibrations in bridges using adaptive tuned mass damper considering human-structure-interaction, Engineering Structures 244 (2021) 112743.

[38] Y. Wang, L. Wang, W. Shi, Two-dimensional air spring based semi-active TMD for vertical and lateral walking and wind-induced vibration control, Structural Engineering and Mechanics 80 (2021) 390.

[39] E. Ahmadi, C. Caprani, S. Živanović, A. Heidarpour, Experimental validation of moving spring-mass-damper model for human-structure interaction in the presence of vertical vibration, Structures 29 (2021) 1274–1285. doi:10.1016/j.istruc.2020.12.007.

[40] M. Zhang, C. T. Georgakis, J. Chen, Biomechanically Excited SMD Model of a Walking Pedestrian, Journal of Bridge Engineering 21 (2016) C4016003.

[41] CEN, Draft prEN 1991-2:2021: Actions on structures — Part 2: Traffic Loads on Bridges and Other Civil Engineering Works, European Committee for Standardization, 2021.

[42] Fiberline Composites A/S, General Design Certification, Fiberline Composites A/S, Middelfart, Denmark, 2018.

Appendix A.

Based on Fiberline Composites A/S [42], characteristic stiffness properties of the FRP elements are presented in Table A.8, in which 'dir. 1' refers to the direction of pultrusion and 'dir. 2' is associated to a direction oriented transversally.

Table A.8: Characteristic stiffness values of FRP elements

Material	Parameter	Symbol	Units	Value
GFRP	Tensile modulus, dir. 1	E_{t1}	GPa	24
	Tensile modulus, dir. 2	E_{t2}	GPa	7
	Compressive modulus, dir. 1	E_{c1}	GPa	24
	Compressive modulus, dir. 2	E_{c2}	GPa	10
	In-plane Poisson's ratio, 12	ν_{12}	-	0.23
	In-plane Poisson's ratio, 21	ν_{21}	-	0.07
	In-plane shear modulus	G_{12}	GPa	3
CFRP	Tensile modulus, direction 1	E_{t1C}	GPa	139

In addition, the density values considered for the GFRP and CFRP are 1800 kg/m^3 and 1550 kg/m^3, respectively, and the geometrical properties of the cross-sections that correspond to the employed FRP elements are listed next:

- I 300x150x15: $h = 300$ mm, $b_f = 150$ mm, $t_w = 15$ mm, $t_f = 15$ mm, $A = 8740$ mm^2, $A_w = 4280$ mm^2, $I_y = 119.0\text{x}10^6$ mm^4, and $I_z = 8.54\text{x}10^6$ mm^4.

- U 300x90x15: $h = 300$ mm, $b_f = 90$ mm, $t_w = 15$ mm, $t_f = 15$ mm, $A = 6850$ mm^2, $A_w = 4050$ mm^2, $I_y = 81.2\text{x}10^6$ mm^4, and $I_z = 4.18\text{x}10^6$ mm^4.

- I 160x80x8: $h = 160$ mm, $b_f = 80$ mm, $t_w = 8$ mm, $t_f = 8$ mm, $A = 2490$ mm^2, $A_w = 1220$ mm^2, $I_y = 9.66\text{x}10^6$ mm^4, and $I_z = 0.69\text{x}10^6$ mm^4.

- SHS 60x60x5: $b = 60$ mm, $t = 5$ mm, $A = 1110$ mm^2, and $I_y = 0.57\text{x}10^6$ mm^4.

- Plank HD: $h = 40$ mm, and $w = 17.06$ kg/m^2.

- CFRP strips: $t_C = 4.9$ mm. The widths of the strips are 150 mm and 90 mm, depending on the width of the flanges of the stringers.

Where h is the depth of the profile, b_f is the flange width, t_w is the web thickness, t_f is the flange thickness, A is the area of the cross-section, A_w is the cross-section area for shear, I_y and I_z are the moments of inertia respect to the major and minor axis, w is the weight of a panel per square meter, and t_C is the thickness of the strip.